Asian Journal of Chemistry; Vol. 23, No. 9 (2011), 4053-4063

ASIAN JOURNAL OF CHEMISTRY

www.asianjournalofchemistry.co.in

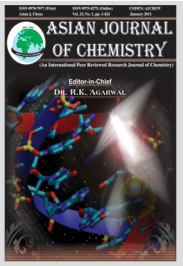

Secondary Organic Aerosol Formation Mechanism by Heterogeneous Reaction of Isoprene with OH Radical: A Theoretical Study

CHENXI ZHANG[1], XIAOMIN SUN[1,2,*] and WENXING WANG[1]

[1]Environment Research Institute, Shandong University, Jinan 250100, P.R. China
[2]State Key Laboratiory of Solid Lubrication, Lanzhou Institute of Chemical Physics, Chinese Academy of Science, Lanzhou 730000, P.R. China

*Corresponding author: Fax: +86 531 88361990; Tel: +86 531 88364416; E-mail: sxmwch@sdu.edu.cn

(*Received*: 27 November 2010; *Accepted*: 18 May 2011) AJC-9967

The comprehensive mechanism of OH-isoprene system is reported. The profile of the potential energy surface was constructed and all of the possible channels were discussed. Geometries have been optimized at the B3LYP level with the 6-31+G** basis set. Part single-point energy calculations have been carried at the QCISD(T)/6-31+G** or B3LYP/6-311++G(3df,2pd) level. Some polyols, for example 2-methylbutanetetraol, are identified, which are easy to take place the aerosol-phase heterogeneous chemical reactions in the formation of secondary organic aerosol. Physical properties such as heats of formation, standard entropies, Gibbs free energies of formation and solvation energies are determined using quantum mechanics method. The quantum mechanics results are used to calculate the equilibrium distributions of the available minima and the equilibrium constants (reported as log K) of aerosol-phase chemical reactions both in gas-phase and aqueous-phase. The results of quantum mechanics calculations are potentially useful in determining the relative thermodynamic tendency for atmospheric aerosol-phase reactions.

Key Words: Isoprene, OH radical, Heterogeneous reaction, Secondary organic aerosol, Quantum mechanics.

INTRODUCTION

Hydrocarbons play an important role in atmospheric chemistry, whose photochemical oxidation results in a number of compounds that have major implications for local and regional air quality, acid deposition and the greenhouse effect[1,2]. Isoprene (2-methyl-1,3-butadiene) is the major biogenic non-methane hydrocarbon, which plays an important role in ozone formation in the local and regional atmosphere due to its high chemical reactivity and importance in the generation of peroxy radicals[2]. It is emitted by a wide variety of plants during daylight as a mechanism to protect plant membranes under conditions of extreme temperature and lack of water[3]. An accurate and complete knowledge of the atmospheric chemistry of isoprene is critical to the elucidation of chemical mechanisms in urban and regional environments. It well known that the atmospheric degradation of isoprene occurs *via* a multi-step chemical process and the reaction with OH is the dominant tropospheric removal pathway.

Normally, the reaction between isoprene and OH occurs primarily by OH addition to the carbon-carbon double bonds resulting in one of four possible isomers. Then adducts react primarily with oxygen molecules under atmospheric conditions to form hydroxyalkyl peroxy radicals and subsequent reaction with NO leads to the formation of hydroxyalkoxy radicals. The dominant tropospheric fate of the hydroxyalkoxy radicals is believed to be decomposition, leading to the formation of various oxygenated and organic nitrate compounds.

A number of groups have studied the OH-initiated oxidation reactions of isoprene. Several laboratory experiments have reported the temperature dependent rate constants of the reaction of isoprene with OH[4-11] and have identified the major reaction products[12-19] which include α,β-unsaturated carbonyls methyl vinyl ketone and methacrolein, formaldehyde and organic nitrates. However, there is also a notable absence of direct experimental data concerning the intermediate processes in the oxidation mechanism, largely due to experimental difficulty to detect the full spectrum of intermediate species and products of the isoprene reactions, although OH cycling experiments have provided indirect information on the intermediate processes. Thus, more and more researches pay attention to the theoretical study. After 2000, North and Zhang and others reported continuously the main final product yields in isoprene oxidation and the subsequence reaction at the CCSD(T)// B3LYP/6-31G** level[20-28]. Claeys *et. al.* observed new polyols *i.e.*, 2-methylthreitol and 2-methylerythritol, in secondary organic aerosols (SOA). The formation mechanism can be explained by OH radical-initiated photooxidation of isoprene[29].

Recently, a possible mechanism for furan formation in the tropospheric oxidation of dienes was proposed in which cyclization of the carbon chain necessarily involves a *cis*-conformation[30].

In this study, we report *ab initio* calculations for the formation of the adduct radicals from the reaction of OH with isoprene and the subsequent reactions. The geometries, energies and physical properties of the main isomers are presented. We also investigate the activation energies against OH migration transforming the higher energy isomers into the lower energy ones. On the basis of *ab initio* calculation, the equilibrium distributions of the main available minima and the equilibrium constants of aerosol-phase chemical reactions including in gas-phase and aqueous-phase are calculated which is helpful to estimate the tendency of the heterogeneous reaction.

Incontestably, the estimation of free energies using quantum methods has some insuperable disadvantages currently. But in the evaluation of thermodynamic tendency of various reactions, the emphasis is not on the absolute but relative changes in the free energies, quantum methods can still provide many useful information, specially for species with no available data.

COMPUTATIONAL METHOD

Geometry optimization: The density functional theory (DFT) becomes a powerful calculation tool in computational chemistry due to the merits in itself[31-34]. In addition, the selection of basis set is of great importance in getting accurate results[35]. This point of view has been widely accepted that the system containing H-bond should adopt the polarization and diffuse functions. Therefore, B3LYP and 6-31+G** are combined to optimize structures at stationary points in all the reaction paths in our work. Reactants, intermediate, transition state and products are investigated through vibrational analysis and at the same time IRC is carried out to determine the correctness of transition states. To test DFT computational results, single point energy calculation is performed using higher-level calculations Quadratic CI calculation including single and double substitutions with a triples correction to the energy [abbreviated as QCISD(T)] with the same basis sets. Relative energy comparison obtained from the above methods is made and the same variational tendency indicates that the results of the DFT method are reliable. All the work is performed using the Gaussian 03 programs[36] and SGI workstation.

Equilibrium distributions: To evaluate the equilibrium distributions of all the available minima qualitatively, the relative Gibbs free energy has been calculated at the room temperatures. The formula used can be described as follows:

$$P_{T(i)} = \frac{e^{-\Delta G_{T(i)}/RT}}{\sum_i e^{-\Delta G_{T(i)}/RT}} \quad (1)$$

where $\Delta G_{T(i)}$ is the Gibbs free energy of isomer i at temperature T relative to the global minimum and R is the ideal gas constant.

Equilibrium constants: To calculate equilibrium constants (K) of the reactions[37], the standard Gibbs free energy of a reaction (ΔG^0_r) which is are needed and can be calculated by the standard Gibbs free energy of formation (ΔG^0_f).The standard Gibbs free energy of a reaction is also related to the equilibrium constant (K) according to the fundamental equation:

$$\Delta G^0_r = \sum_j v_j \Delta G^0_{f,j} = -RT \ln K \quad (2)$$

where v_j is the stoichiometric coefficient for j in the reaction and $\Delta G^0_{f,j}$ is the standard Gibbs free energy of formation for j. $\Delta G^0_{f,j}$ can be determined using gas-phase heats of formations and standard entropies ($\Delta G^0_{f,j} = \Delta H^0_{f,j} - T\Delta S^0_{f,j}$). Then, as illustrated by **Scheme-I**, the free energy of reaction in aqueous solution, $\Delta G^0_r(aq)$ is related to the gas-phase free energy of reaction, $\Delta G^0_r(gas)$ by adding the solvation energies of the species, ΔG^0_s.

$$\Delta G^0_r(aq) = \Delta G^0_r(gas) + \sum_j v_j \Delta G^0_s \quad (3)$$

All the necessary quantities ($\Delta G^0_{f,j}$, ΔS^0_j and ΔG^0_s) can be determined by quantum mechanics, It should be noted here that proper standard state conditions should be used for the free energy calculations in eqn. 3. The standard state for gas-phase reactions is 1.0 atm at 298.15 K, while the standard state for aqueous solution is 1.0 mol/L at 298.15 K.

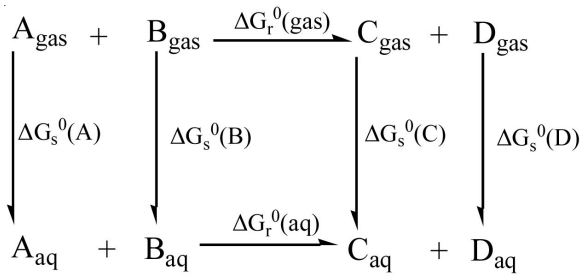

Scheme-I: Thermodynamic cycle for computation of Gibbs free energy changes of reaction in the gas phase and solution

As for the gas-phase standard heats of formation, Gibbs free energies of formation and solution-phase energy, the calculated methods are discussed[37]. It should be pointed out that the polarized continuum model (PCM)[38,39] is chosen to calculate the solvation energy. The solvation energy (ΔG^0_s) describes the interaction of a solute with a surrounding solvent. The polarized continuum model have proved flexible and accurate, in particular, when the solute is accommodated in a cavity of realistic molecular shape and has been widely used for the study of many chemical processes. Water is chosen in this study because it is often the most important component in aerosols. Once solvation energies, ΔG^0_s, for both the parent compounds and reaction products are obtained, the equilibrium constants of the solution reactions can be calculated.

RESULTS AND DISCUSSION

Isomerization of *trans*/*cis*-isoprene: It is not difficult to find two isomers of isoprene, usually labeled *trans*-isoprene and *cis*-isoprene. The *trans*-isoprene is more stable than the *cis*-isoprene from the aspect of energy. However, the *cis*-isoprene may also exit stably. What's more it is one of the important reagents in the Diels-Alder synthesis reaction. The *trans*-isoprene could be converted into the *cis*-isoprene after

passing the potential barrier 4.69 kcal/mol. The energy of the *cis*-isoprene relative to that of the *trans*-isoprene is +3.40 kcal/mol. In the geometry of the transition state, the dihedral angle ∠C1C4C5C7 is -103.1°. The geometry parameters of the *trans*-isoprene, the transition state and the *cis*-isoprene is listed in Fig. 1. It can be seen that the *trans*-isoprene has a planar structure while *cis*-isoprene and the isomerization transition state have non-planar ones. At the room temperature, the equilibrium distribution of *cis*-isoprene/*trans*-isoprene is about 0.05:0.95. Since the reaction between isoprene with -OH takes place during the daylight and the isomerization barrier between the *trans*-isoprene and the *cis*-isoprene is not high, the reactions of both the *trans*-isoprene and the *cis*-isoprene with -OH should be taken into account when the mechanism is studied. 3-Methylfuran is one of the products in the OH-initiated oxidation reactions of isoprene. Recently, a possible mechanism for furan formation was proposed in which the framework of furan results from the *cis*-isoprene.

Addition reaction of OH-initiated reactions: Since the addition of OH to the double bonds of isoprene proceeds without a barrier, the abundant energy adducts can be obtained directly. It has been widely accepted that -OH may add to any of the four carbon atoms of *trans*/*cis*-isoprene to form hydroxyl alkyl radicals. Subsequently, hydroxyl alkyl radicals can react with -OH radical till to the formation of methylbutanetetraols passing through methylbutenediols and methylbutanetriol radicals. Methylbutanetetraols have been observed in experiment. All the possible reaction paths of *trans*/*cis*-isoprene with OH radicals are given in Fig. 2. For the sake of convenience, the adducts are labeled *t*- or *c*-according to the carbon skeleton coming from the *trans*- or *cis*-isoprene and the Arabian numbers are the adding position of OH group to the isoprene molecule. For example, the label *t*-1 implies that the OH group is added to the C1 position of *trans*-isoprene.

Methylbuteneol radicals: In the first step, when -OH is added to the *t*/*c*-isoprene, four groups of adducts is formed because of the different adding positions which are labeled *t*/*c*-1, *t*/*c*-2, *t*/*c*-3 and *t*/*c*-4, respectively. Those adducts belong to the alkene-ol compounds. Because of the stereochemistry of OH group, every adduct of each position has three isomers which are labeled as a, b and c. The transformation of different isomers between both the same adding position and different adding position can be occurred easily, which deepen the complexity of the reaction paths. The schematic potential energy surfaces of the reactions *t*/*c*-isoprene with OH are drawn

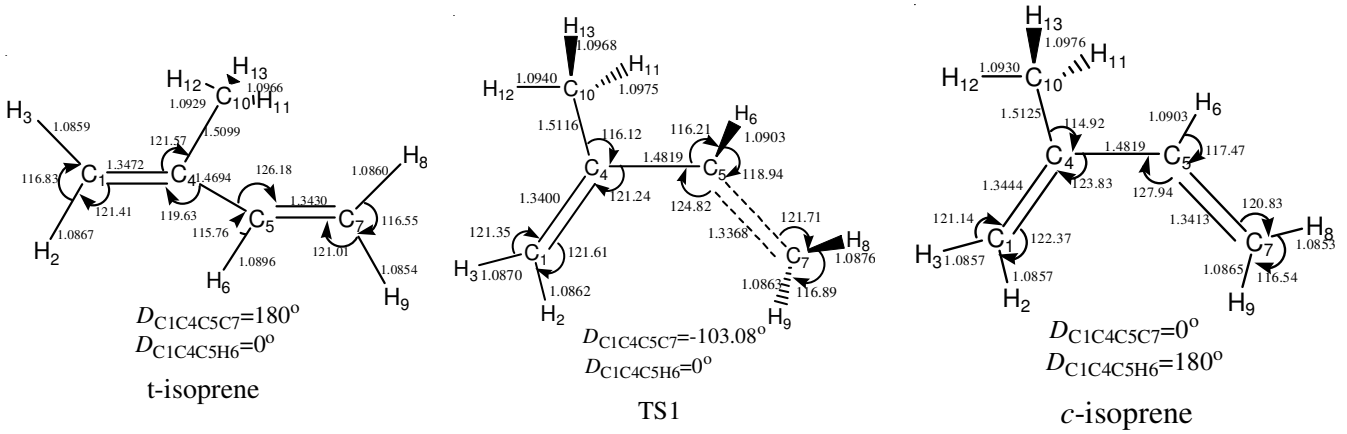

Fig. 1. The geometry parameters of the *trans*/*cis*-isoprene and the isomerization transition state at the B3LYP/6-31+G** level

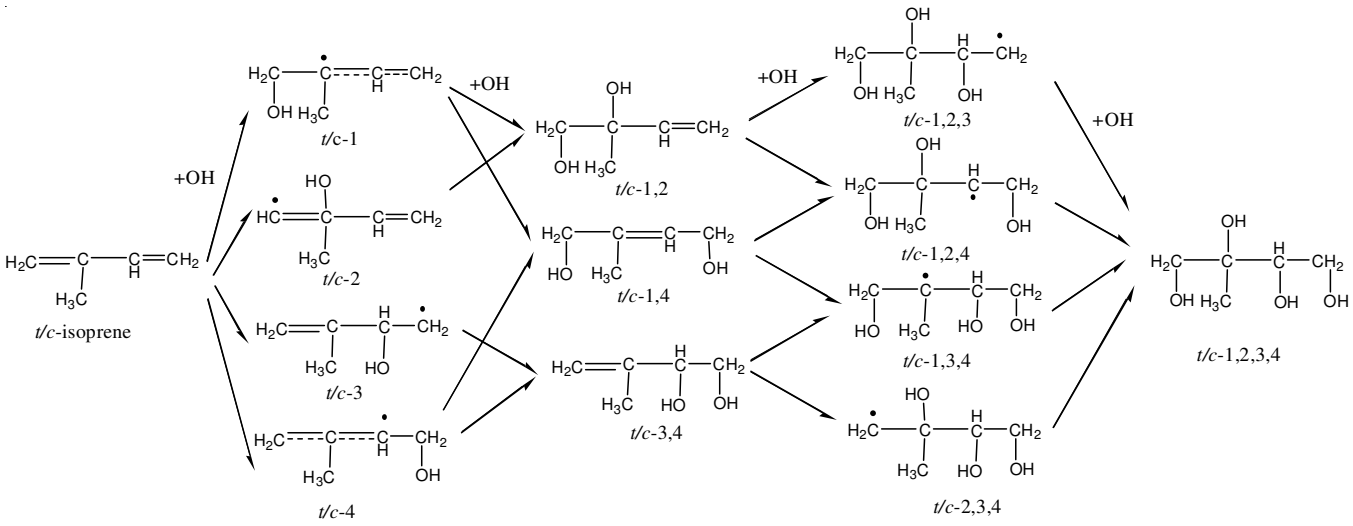

Fig. 2. Schematic reaction paths of isoprene with OH radical (a) *trans*-isoprene -OH adducts, (b) *cis*-isoprene -OH adducts

in Fig. 3(a) and (b), respectively. The thermochemistry constants of the stationary points and selected geometric parameters of stationary points are listed from Tables 1 and 2. The detailed discussion taking C1 position in *t*-isoprene for example is as following.

(1) Adding to C1 carbon atom: When OH is added to the C1 atom of *t*-isoprene, products *t*-1a, *t*-1b and *t*-1c can be obtained whose energies are -37.82,-36.52 and -36.26 kcal/mol relative to that of OH + *t*-isoprene, respectively. At 298.15 K, the equilibrium distribution is 0.62:0.28:0.10. These three products can be converted into each other. After passing transition state *t*-TS1a, *t*-1a can be changed into *t*-1b with the potential barrier 2.30 kcal/mol. *t*-1b may be changed into *t*-1c after going through the potential barrier 0.85 kcal/mol, which corresponds to the transition state *t*-TS1c. If passing the transition state *t*-TS1b with the potential barrier 3.63 kcal/mol,

TABLE-1
TOTAL ENERGIES (a.u.), ZPVE (a.u.), ENTHALPIES (a.u.), GIBBS FREE ENERGIES (a.u.), ENTROPY (cal/(mol .k)), HEAT CAPACITIES (cal/(mol .k)), PARTITION FUNCTION, ROTATIONAL CONSTANTS (GHZ) AND DIPOLE MOMENTS (Debye) OF STATIONARY POINTS ON THE REACTIONS OF OH ADDING TO C1 TO C4 POSITION

		C1-position						C2-position					
		t-P1a	*t*-P1b	*t*-P1c	*t*-TS1a	*t*-TS1b	*t*-TS1c	*t*-P2a	*t*-P2b	*t*-P2c	*t*-TS2a	*t*-TS2b	*t*-TS2c
trans-	E_{total}	-271.00830	-271.00680	-271.00605	-271.00560	-271.00379	-271.00538	-270.97983	-270.98103	-270.98096	-270.97952	-270.97849	-270.97909
	ZPE	0.12794	0.12742	0.12753	0.12703	0.12716	0.12713	0.12557	0.12591	0.12587	0.12505	0.12510	0.12499
	H[a]	-270.99968	-270.99889	-270.99722	-270.99732	-270.99578	-270.99709	-270.97089	-270.97234	-270.97226	-270.97112	-270.97016	-270.97067
	G[a]	-271.04063	-271.03989	-271.03887	-271.03780	-271.03513	-271.03765	-271.01166	-271.01235	-271.01227	-271.01086	-271.00960	-271.01045
	S	86.194	88.263	87.652	85.205	82.827	85.355	85.819	84.199	84.205	83.643	83.004	83.717
	C_v	26.835	27.075	27.088	25.353	25.193	25.268	28.978	28.689	28.779	27.200	27.185	27.238
	Q	0.106D-43	0.406D-43	0.273D-43	0.208D-43	0.840D-43	0.231D-43	0.765D-43	0.312D-43	0.321D-43	0.789D-43	0.589D-43	0.850D-43
	A[b]	6.6217	6.8822	6.5411	6.8486	7.7531	6.2279	4.7580	4.6839	4.6838	4.7107	4.6769	4.6614
	B[b]	2.1346	2.1259	2.1443	2.1184	2.0585	2.1816	2.8063	2.8422	2.8275	2.8132	2.8217	2.8245
	C[b]	1.7736	1.7624	1.7757	1.7545	1.6675	1.8016	2.6649	2.7040	2.6988	2.6769	2.6996	2.7071
	D[c]	1.4226	1.7209	2.0597	1.5780	1.9446	1.9697	1.5721	1.7558	1.7232	1.7216	1.8236	1.7131
		c-P1a	*c*-P1b	*c*-P1c	*c*-TS1a	*c*-TS1b	*c*-TS1c	*c*-P2a	*c*-P2b	*c*-P2c	*c*-TS2a	*c*-TS2b	*c*-TS2c
cis-	E_{total}	-271.00563	-271.00689	-271.00484	-271.00469	-271.00501	-271.00476	-270.98039	-270.98099	-270.97853	-270.97963	-270.97855	-270.97723
	ZPE	0.12758	0.12795	0.12750	0.12706	0.12724	0.12707	0.12547	0.12589	0.12499	0.12499	0.12475	0.12503
	H[a]	-270.99692	-270.99828	-270.99604	-270.99643	-270.99685	-270.99650	-270.97149	-270.97225	-270.96940	-270.97128	-270.97006	-270.96885
	G[a]	-271.03804	-271.03920	-271.03787	-271.03697	-271.03673	-271.03699	-271.01215	-271.01257	-271.01080	-271.01080	-271.01012	-271.00862
	S	86.534	86.113	88.045	85.322	83.941	85.213	85.581	84.851	87.133	83.179	84.312	83.716
	C_v	27.036	26.880	27.140	25.358	25.211	25.342	28.928	28.658	29.236	27.160	27.290	27.067
	Q	0.167D-43	0.101D-43	0.355D-43	0.255D-43	0.116D-43	0.240D-43	0.783D-43	0.414D-43	0.224D-43	0.705D-43	0.137D-43	0.847D-43
	A[b]	5.2254	4.5049	5.0172	5.0958	3.6754	5.1272	4.7324	4.8247	4.7229	4.7434	4.7159	4.7831
	B[b]	2.5373	2.7613	2.5626	2.5533	3.4514	2.5370	2.7509	2.7432	2.7587	2.7421	2.7560	2.7400
	C[b]	1.8144	1.8884	1.8106	1.8171	1.9737	1.8094	2.7344	2.6804	2.7072	2.7130	2.7164	2.6930
	D[c]	1.5770	1.5169	2.1009	1.1568	2.1104	1.9628	1.7723	1.4347	1.8009	1.6267	1.7531	1.9909
		C3-position						C4-position					
		t-P3a	*t*-P3b	*t*-P3c	*t*-TS3a	*t*-TS3b	*t*-TS3c	*t*-P4a	*t*-P4b	*t*-P4c	*t*-TS4a	*t*-TS4b	*t*-TS4c
trans-	E_{total}	-270.98299	-270.98252	-270.98247	-270.98081	-270.98018	-270.97954	-271.00458	-271.00401	-271.00332	-271.00324	-271.00234	-271.00227
	ZPE	0.125794	0.12621	0.12628	0.12512	0.12532	0.12500	0.12779	0.12782	0.12718	0.12724	0.126944	0.12703
	H[a]	-270.97393	-270.97367	-270.97364	-270.97222	-270.97170	-270.97087	-270.99602	-270.99544	-270.99460	-270.99511	-270.99413	-270.99407
	G[a]	-271.01547	-271.01454	-271.01446	-271.01280	-271.01195	-271.01197	-271.03691	-271.03612	-271.03623	-271.03519	-271.03473	-271.03467
	S	87.413	86.020	85.916	84.412	82. 694	86.493	86.074	85.604	87.616	84.365	85.458	85.446
	C_v	28.479	28.268	28.238	26.879	26.794	26.848	26.915	26.971	27.146	25.258	25.383	25.332
	Q	0.127D-42	0.474D-43	0.427D-43	0.145D-42	0.930D-43	0.262D-42	0.124D-43	0.945D-44	0.437D-43	0.148D-43	0.323D-43	0.297D-43
	A[b]	4.7295	4.7073	4.7074	4.6894	4.6689	4.7022	7.1227	6.4827	7.5239	6.6294	7.2034	7.1810
	B[b]	2.6454	2.7562	2.7533	2.7031	2.7005	2.6188	1.9221	2.2008	1.8957	2.0586	1.9147	1.9180
	C[b]	2.5487	2.4951	2.4971	2.5125	2.4915	2.5358	1.6248	1.8561	1.5678	1.7699	1.6147	1.6193
	D[c]	1.4886	1.5071	1.9857	1.2004	1.8664	2.0760	1.9741	1.7001	2.1528	1.9628	1.9680	2.1527
		c-P3a	*c*-P3b	*c*-P3c	*c*-TS3a	*c*-TS3b	*c*-TS3c	*c*-P4a	*c*-P4b	*c*-P4c	*c*-TS4a	*c*-TS4b	*c*-TS4c
cis-	E_{total}	-270.98058	-270.98086	-270.98136	-270.97954	-270.97853	-270.97854	-271.00313	-271.00431	-271.00346	-271.00273	-271.00246	-271.00243
	ZPE	0.12649	0.12611	0.12593	0.12559	0.12499	0.12499	0.12752	0.12754	0.13487	0.12695	0.12636	0.12642
	H[a]	-270.97180	-270.97203	-270.97246	-270.97117	-270.96992	-270.96993	-270.99433	-270.99552	-270.99449	-270.99436	-270.99397	-270.99397
	G[a]	-271.01270	-271.01289	-271.01341	-271.01125	-271.01084	-271.01086	-271.03609	-271.03783	-271.03732	-271.03582	-271.03591	-271.03559
	S	86.079	85.986	86.189	84.356	86.134	86.145	87.880	89.066	90.156	87.250	88.263	87.588
	C_v	28.145	28.271	28.404	26.596	26.821	26.823	27.107	27.035	27.350	25.375	25.625	25.615
	Q	0.391D-43	0.528D-43	0.661D-43	0.658D-43	0.235D-43	0.238D-43	0.320D-43	0.570D-43	0.171D-43	0.666D-43	0.182D-43	0.126D-43
	A[b]	4.7911	4.7670	4.8460	4.7696	4.7696	4.8398	7.0333	7.4350	7.9689	7.0316	7.9725	7.9770
	B[b]	3.1458	3.2017	2.9488	3.2149	3.2149	2.9164	2.1131	1.8604	1.8355	2.0222	1.8158	1.8158
	C[b]	2.0937	2.1117	2.2282	2.0855	2.0855	2.2030	1.7990	1.6014	1.5207	1.7687	1.5122	1.5120
	D[c]	1.6450	1.4928	2.0489	1.3556	1.7778	1.8772	2.0699	2.1363	1.6297	2.3722	1.6106	1.9244

[a]The data including ZPVE corrections; [b]A; B and C are rotational constants; [c]D refers to dipole moments.

t-1a will be turned into *t*-1c. It is the stereochemistry of OH group that result in those three isomers. The position of OH group can be observed from the change of dihedral angle $\angle H_2C_1O_{14}H_{15}$. In the process *t*-1a → *t*-TS1a → *t*-1b → *t*-TS1c → *t*-1c, dihedral angle $\angle H_2C_1O_{14}H_{15}$ varies conforming to the sequence 63.47°→-9.6°→-69.6° →-116.8°→-169.9° and at the transition state *t*-TS1b the number is 138.4°.

The adding reaction paths on other C atoms are similar to those on C1 atom in *t*-isoprene.

(2) OH migration reaction of the OH-*t*-isoprene adducts: Among the OH-*t*-isoprene adducts, isomers result from different carbon atom can interconvert. For example, the isomers of C1 position can convert to those of C2 position and the isomers of C3 position can convert to those of C4 position. The transition states for OH migration have also been investigated which are identified at the B3LYP/6-31+G** level and the single point energy calculations for the transition states were performed at the QCISD(T)/6-31+G** level. There are

TABLE-2
SELECTED GEOMETRIC PARAMETERS OF STATIONARY POINTS ON THE REACTION OF OH ADDING TO C1 TO C4 POSITION

	C1-position							C2-position					
	t-P1a	*t*-P1b	*t*-P1c	*t*-TS1a	*t*-TS1b	*t*-TS1c		*t*-P2a	*t*-P2b	*t*-P2c	*t*-TS2a	*t*-TS2b	*t*-TS2c
R_{C1C4}	1.5047	1.5014	1.5042	1.5034	1.5197	1.5018	R_{C4O14}	1.4676	1.4471	1.4456	1.4677	1.4495	1.4514
R_{C1O14}	1.4386	1.4387	1.4406	1.4440	1.4247	1.4463	R_{C1C4}	1.4979	1.5006	1.4969	1.4974	1.5011	1.5018
R_{O14H15}	0.9671	0.9659	0.9660	0.9636	0.9655	0.9657	R_{O14H15}	0.9681	0.9681	0.9678	0.9669	0.9646	0.9660
R_{C4C5}	1.4022	1.3987	1.4003	1.3984	1.4017	1.4025	R_{C4C5}	1.5176	1.5194	1.5244	1.5192	1.5236	1.5214
R_{C5C7}	1.3846	1.3853	1.3834	1.3858	1.3818	1.3818	R_{C5C7}	1.3349	1.3372	1.3384	1.3358	1.3374	1.3375
$A_{O14C1C4}$	112.99	109.33	113.49	110.51	115.22	113.50	$A_{O14C4C5}$	108.23	104.43	108.13	106.54	105.91	109.28
$A_{O14C1H2}$	110.52	110.51	105.05	110.89	105.12	106.28	$A_{O14C4C1}$	108.54	109.77	106.01	109.64	107.87	109.12
A_{C1C4C5}	119.79	119.53	120.03	119.78	117.42	120.08	A_{C1C4C5}	109.97	106.81	107.14	108.59	107.16	107.06
A_{C4C5C7}	127.09	127.77	127.25	127.67	127.96	126.50	A_{C4C5C7}	127.44	127.03	127.35	127.28	127.40	127.39
$D_{H15O14C1C4}$	-59.07	168.84	69.04	-132.05	72.17	16.18	$D_{H15O14C4C1}$	52.98	-51.29	170.46	11.27	-121.19	99.88
$D_{O14C1C4C5}$	119.94	124.02	112.87	126.30	174.19	103.86	$D_{O14C4C5C7}$	-118.34	-165.49	-131.55	-124.24	-140.24	-125.63
$D_{C1C4C5C7}$	177.49	176.78	179.01	176.55	177.16	178.84	$D_{C1C4C5C7}$	123.25	106.52	114.58	117.74	104.80	116.31
	c-P1a	*c*-P1b	*c*-P1c	*c*-TS1a	*c*-TS1b	*c*-TS1c		*c*-P2a	*c*-P2b	*c*-P2c	*c*-TS2a	*c*-TS2b	*c*-TS2c
R_{C1C4}	1.5018	1.5055	1.5070	1.5046	1.5077	1.5049	R_{C4O14}	1.4615	1.4502	1.4480	1.4704	1.4520	1.4648
R_{C1O14}	1.4363	1.4411	1.4361	1.4421	1.4442	1.4401	R_{C1C4}	1.4962	1.4969	1.4943	1.494	1.4958	1.4972
R_{O14H15}	0.9655	0.9669	0.9654	0.9633	0.9657	0.9634	R_{O14H15}	0.9680	0.9679	0.9671	0.9666	0.9660	0.9672
R_{C4C5}	1.3998	1.4014	1.3998	1.3994	1.4034	1.4002	R_{C4C5}	1.5178	1.5212	1.5274	1.5182	1.5257	1.5184
R_{C5C7}	1.3856	1.3861	1.3856	1.3863	1.3836	1.3857	R_{C5C7}	1.3340	1.3358	1.3343	1.3346	1.3349	1.3348
$A_{O14C1C4}$	109.08	112.37	113.79	110.44	113.66	111.79	$A_{O14C4C5}$	103.52	107.79	108.65	105.13	108.79	107.28
$A_{O14C1H2}$	110.32	110.26	105.03	110.60	106.78	107.33	$A_{O14C4C1}$	108.76	109.89	105.63	109.27	106.70	105.58
A_{C1C4C5}	122.44	122.69	122.76	122.71	121.19	122.59	A_{C1C4C5}	113.71	114.33	113.62	113.50	113.73	113.67
A_{C4C5C7}	128.55	128.24	128.35	128.50	126.70	128.47	A_{C4C5C7}	126.24	127.46	127.07	126.64	126.82	126.76
$D_{H15O14C1C4}$	172.72	-60.02	72.06	-129.69	5.11	112.63	$D_{H15O14C4C1}$	-55.76	63.26	171.98	-6.39	140.26	-139.45
$D_{O14C1C4C5}$	136.03	110.19	128.55	133.63	71.37	131.29	$D_{O14C4C5C7}$	141.16	116.83	114.74	143.05	113.08	134.66
$D_{C1C4C5C7}$	-2.72	0.73	-2.81	-1.60	0.56	-2.49	$D_{C1C4C5C7}$	23.34	-5.66	-2.50	23.69	-5.68	18.34
	C3-position							C4-position					
	t-P3a	*t*-P3b	*t*-P3c	*t*-TS3a	*t*-TS3b	*t*-TS3c		*t*-P4a	*t*-P4b	*t*-P4c	*t*-TS4a	*t*-TS4b	*t*-TS4c
R_{C5O14}	1.4368	1.4395	1.4457	1.4431	1.4355	1.4402	R_{C7O14}	1.4382	1.4458	1.4326	1.4503	1.4424	1.4429
R_{O14H15}	0.9667	0.9670	0.9675	0.9634	0.9665	0.9646	R_{C1C4}	1.3890	1.3858	1.3885	1.3876	1.3886	1.3887
R_{C1C4}	1.3400	1.3396	1.3384	1.3390	1.3391	1.3388	R_{O14H15}	0.9671	0.9670	0.9656	0.9661	0.9640	0.9640
R_{C4C5}	1.5321	1.5266	1.5232	1.5300	1.5332	1.5291	R_{C4C5}	1.4022	1.4056	1.3999	1.4044	1.4012	1.4012
R_{C5C7}	1.4899	1.4945	1.4941	1.4947	1.4958	1.4956	R_{C5C7}	1.4949	1.4990	1.4926	1.4945	1.4944	1.4942
$A_{O14C5C4}$	107.34	107.34	111.91	108.91	111.73	112.50	$A_{O14C7C5}$	112.22	113.31	108.20	112.84	110.84	110.84
$A_{O14C5H6}$	109.68	109.68	103.35	109.87	104.57	105.41	$A_{O14C7H8}$	110.45	104.08	110.69	107.03	109.51	107.60
A_{C1C4C5}	119.93	119.93	120.28	120.29	120.17	120.28	A_{C1C4C5}	120.15	120.35	120.48	120.15	120.21	120.18
A_{C4C5C7}	111.60	111.60	113.05	112.17	111.37	112.63	A_{C4C5C7}	126.77	124.62	125.80	125.63	126.53	126.55
$D_{H15O14C5C4}$	57.14	-171.07	-84.98	124.00	-79.80	-18.41	$D_{H15O14C7C5}$	-53.16	52.87	170.63	2.38	-114.01	114.04
$D_{O14C5C4C1}$	-118.97	-130.00	-123.93	-128.48	-124.99	-116.09	$D_{O14C7C5C4}$	130.57	72.41	152.41	96.26	62.00	126.76
$D_{C1C4C5C7}$	120.51	107.76	110.14	109.98	108.51	118.64	$D_{C1C4C5C7}$	179.70	-177.70	177.65	-177.91	-129.55	179.61
	c-P3a	*c*-P3b	*c*-P3c	*c*-TS3a	*c*-TS3b	*c*-TS3c		*c*-P4a	*c*-P4b	*c*-P4c	*c*-TS4a	*c*-TS4b	*c*-TS4c
R_{C5O14}	1.4608	1.4469	1.4449	1.4645	1.4433	1.4433	R_{C7O14}	1.4414	1.4376	1.4300	1.4478	1.4331	1.4331
R_{O14H15}	0.9687	0.9668	0.9658	0.9665	0.9653	0.9653	R_{C1C4}	1.3844	1.3894	1.3847	1.3855	1.3844	1.3845
R_{C1C4}	1.3400	1.3383	1.3381	1.3392	1.3386	1.3386	R_{O14H15}	0.9668	0.9670	0.9650	0.9658	0.9631	0.9631
R_{C4C5}	1.5235	1.5282	1.5281	1.5239	1.5945	1.5945	R_{C4C5}	1.4066	1.4024	1.4027	1.4068	1.4040	1.4037
R_{C5C7}	1.4899	1.4904	1.4901	1.4890	1.4875	1.4875	R_{C5C7}	1.5023	1.4961	1.4954	1.4978	1.4992	1.4993
$A_{O14C5C4}$	110.28	106.12	106.02	108.20	111.08	111.08	$A_{O14C7C5}$	114.32	112.00	107.88	113.36	110.49	110.48
$A_{O14C5H6}$	102.32	108.44	108.24	105.44	107.56	107.56	$A_{O14C7H8}$	109.90	104.30	110.43	107.56	107.91	110.69
A_{C1C4C5}	122.91	122.24	122.14	122.54	122.21	122.21	A_{C1C4C5}	122.45	123.97	122.62	122.85	122.59	122.58
A_{C4C5C7}	116.65	116.21	116.11	115.87	115.67	115.67	A_{C4C5C7}	125.11	127.21	125.09	125.25	125.16	125.10
$D_{H15O14C5C4}$	71.80	-178.86	-53.16	127.90	-115.91	-115.91	$D_{H15O14C7C5}$	-48.61	55.53	-129.08	-3.37	119.75	-120.02
$D_{O14C5C4C1}$	-131.09	-129.45	-129.35	-137.11	-101.40	-101.40	$D_{O14C7C5C4}$	-65.06	-128.04	-176.1	-84.18	174.10	-176.23
$D_{C1C4C5C7}$	-5.80	-6.07	-6.007	-13.05	21.84	21.84	$D_{C1C4C5C7}$	1.51	0.56	0.63	0.34	0.22	-0.70

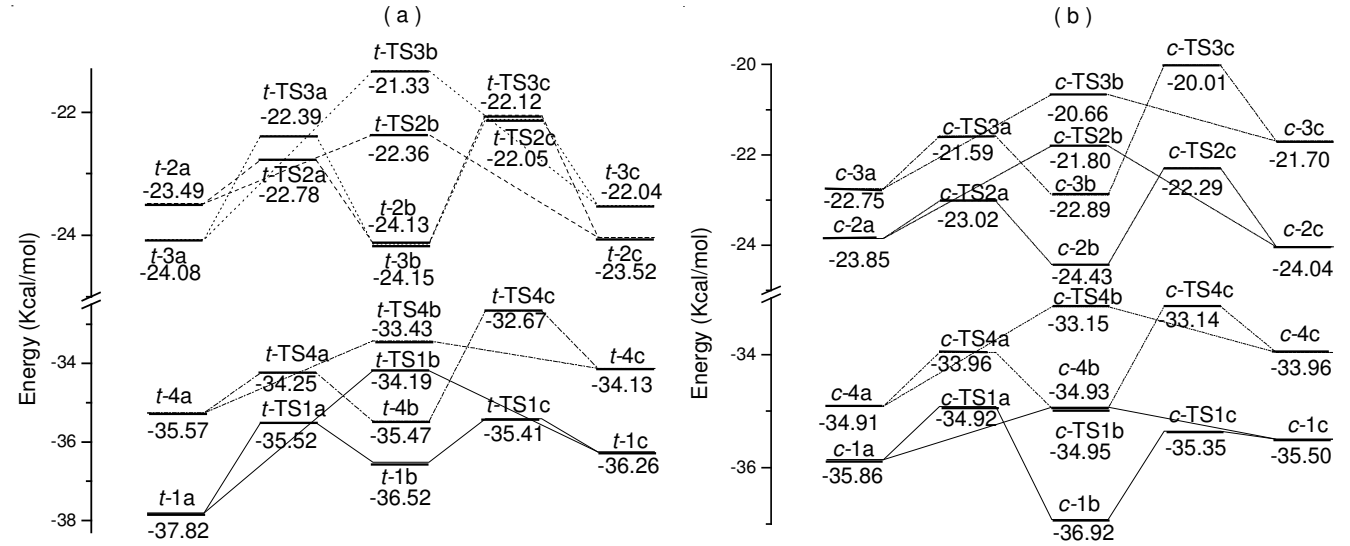

Fig. 3. Schematic potential energy surfaces of transformation reaction among the adducts at the QCISD(T)||B3LYP/6-31+G** level (a) *trans*-isoprene -OH adducts, (b) *cis*-isoprene -OH adducts

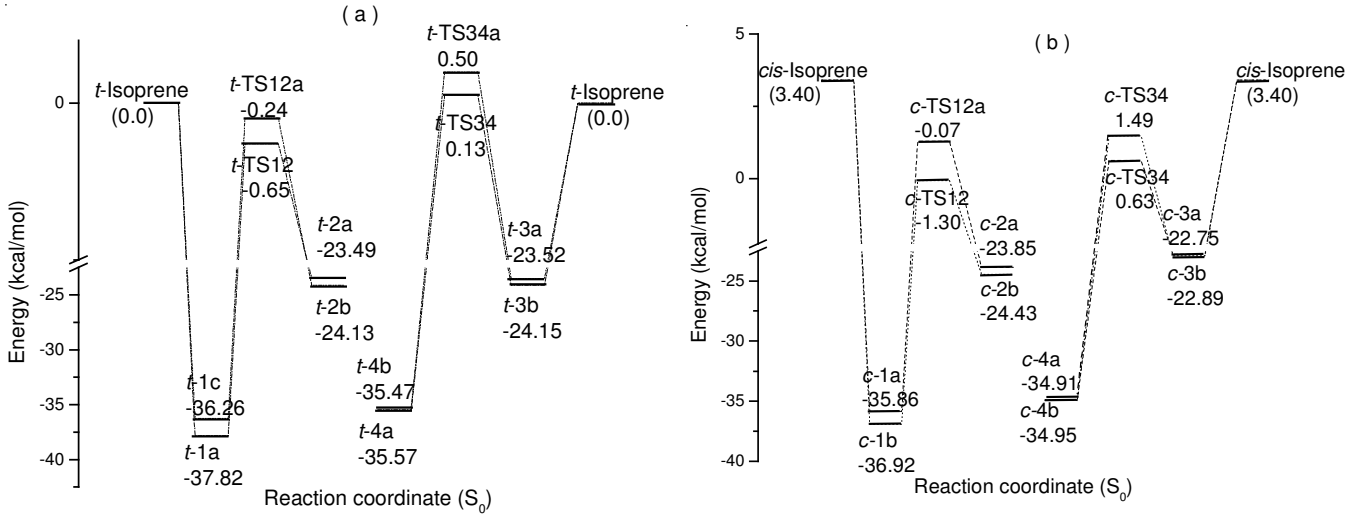

Fig. 4. Schematic potential energy surfaces for OH migration reactions at the QCISD(T)||B3LYP/6-31+G** level (a) *trans*-isoprene -OH adducts, (b) *cis*-isoprene -OH adducts

four transition states. The schematic potential energy surfaces for OH migration of the *t*-isoprene-OH adducts are drawn in Fig. 4(a). The geometry parameters of the OH migration transition states are shown in Fig. 5(a). The transition state which associates with the interconversion of isomers *t*-1a and *t*-2a labeled *t*-TS12 is located 37.17 kcal/mol above isomer *t*-1a. The transition state between isomers *t*-1c and *t*-2b labeled *t*-TS12a is located 36.02 kcal/mol above isomer *t*-1c. The transition state *t*-TS34 associated with isomers *t*-4a and *t*-3a is located 35.7 kcal/mol above isomer *t*-4a. The transition state *t*-TS34a between isomers *t*-4b and *t*-3b is located 35.97 kcal/mol above isomer *t*-4b. It is obvious that each OH migration reaction has a comparable high barrier. However the abundant energy adducts can be obtained directly for the reaction of OH-*t*-isoprene proceeds without a barrier. Compared to the energy of OH and *t*-isoprene, the transition state *t*-TS12 and *t*-TS12a are located -0.65 and -0.24 Kcal/mol, respectively, while the energies of transition states *t*-TS34 and *t*-TS34a are higher 0.13 and 0.50 Kcal/mol than that of -OH and *t*-isoprene. It can be seen that the -OH migration reaction is easy to occur.

The paths of adding reaction and migration reaction in *c*-isoprene are similar to those in *t*-isoprene which are shown in Fig. 3(b) and 4(b), respectively. The geometry parameters of the OH migration transition states are shown in Fig. 5(b). As illustrated in Fig. 3, *c*-1b, *c*-2b, *c*-3b, *c*-4b, *t*-1a, *t*-2b, *t*-3b and *t*-4a are the compounds with the lowest energy on each adding position, *i.e.*, they are the most stable structures on each position. Especially, the energies of *c*-1b and *c*-4b are lower than those of *c*-2b and *c*-3b and the energies of *t*-1a and *t*-4a are lower than those of *t*-2b and *t*-3b. Obviously, the terminal isomers are considerably more stable than the others since addition at the corresponding carbons allows the radical center to be delocalized. For the subsequent step, only the most stable structure on each step whose main geometry parameters are drawn in Fig. 6 is reported though all the isomers are calculated. The completed potential energy surfaces to form the polyols are drawn in Fig. 7.

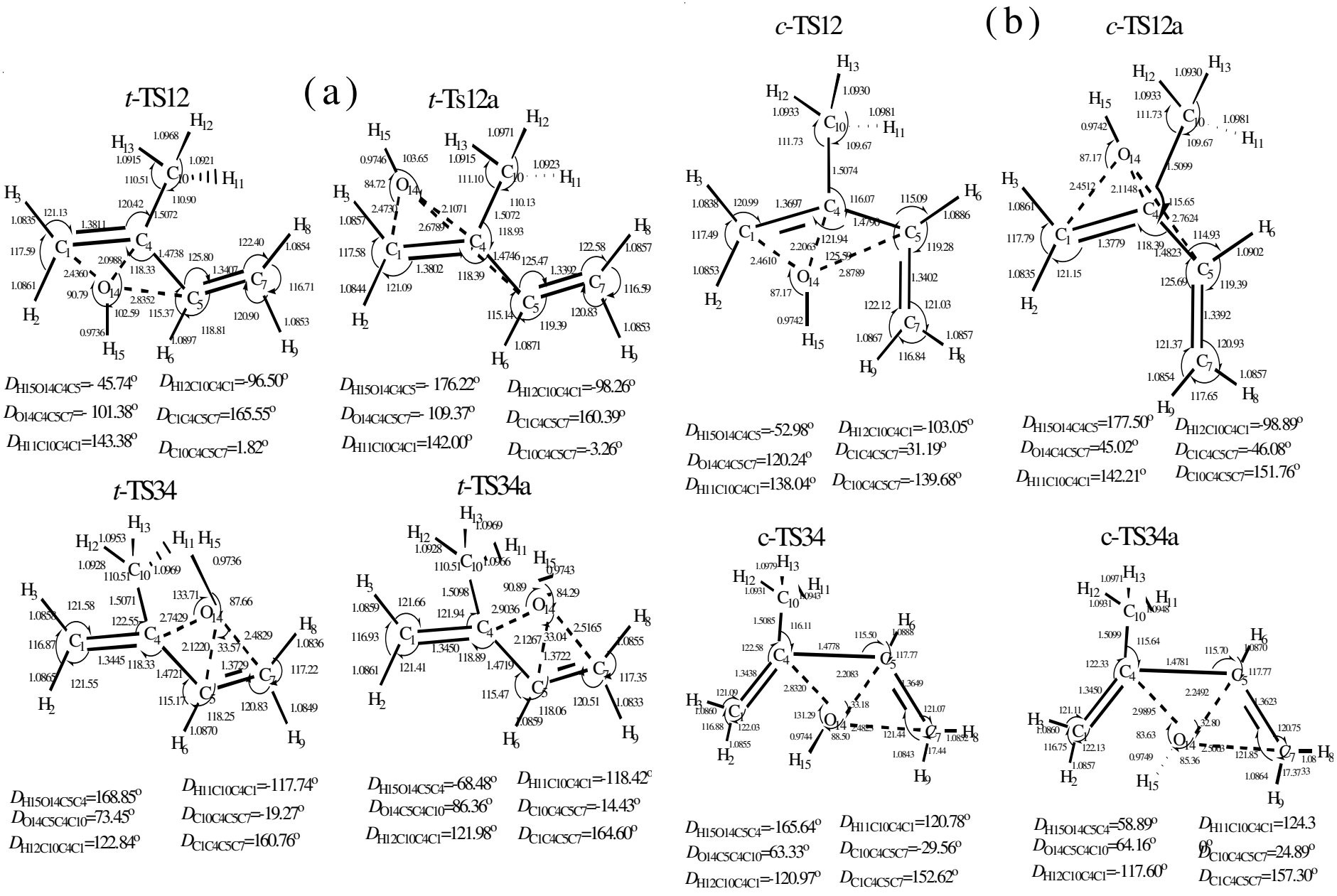

Fig. 5. The geometry parameters of OH migration transition states at the B3LYP/6-31+G** level (a) *trans*-isoprene -OH adducts, (b) *cis*-isoprene -OH adducts

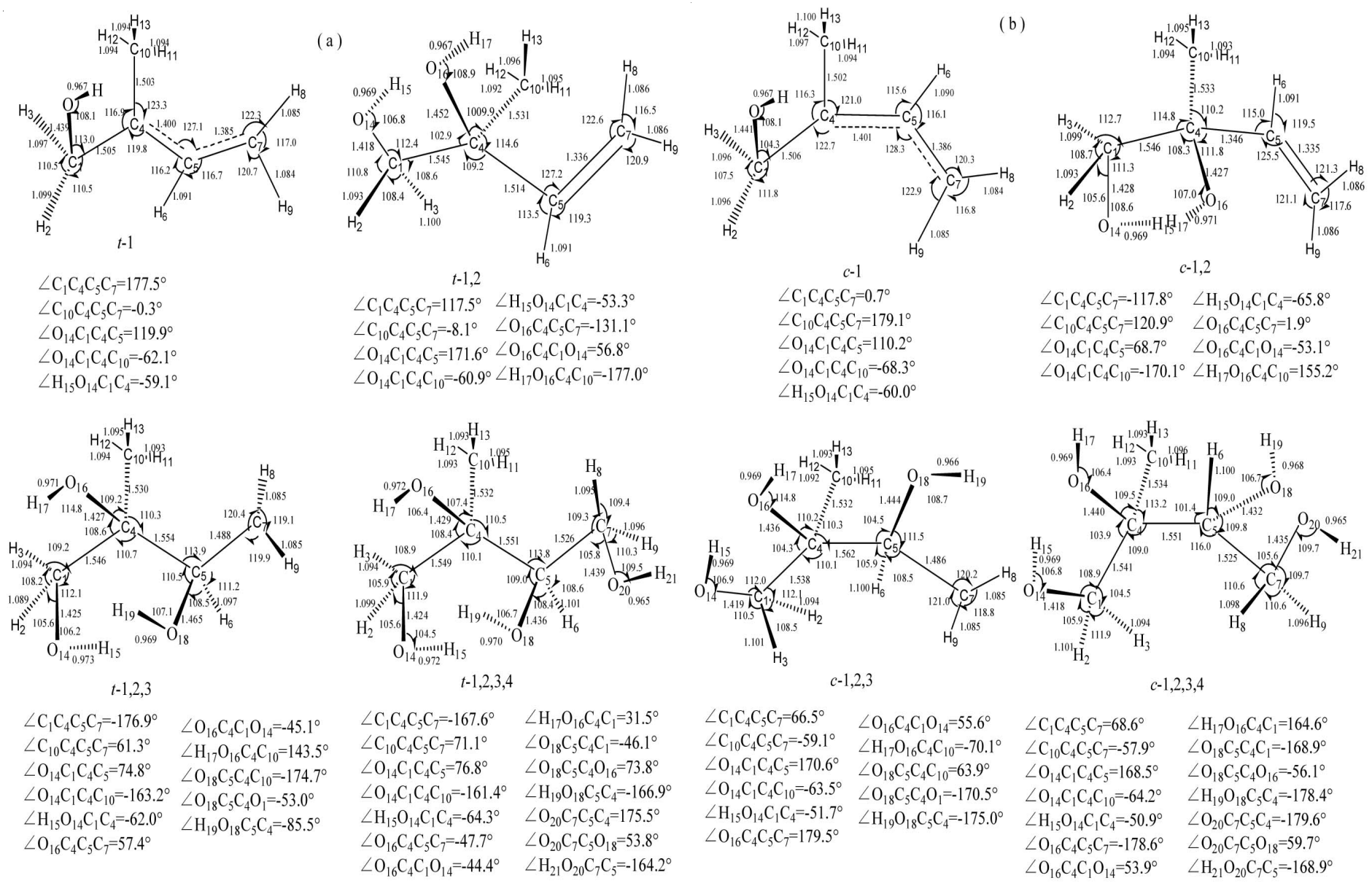

Fig. 6. The geometry parameters of stationary points of the multi-step addition reaction at the B3LYP/6-31+G** level (a) The system of *trans*-isoprene with OH, (b) The system of *cis*-isoprene with OH

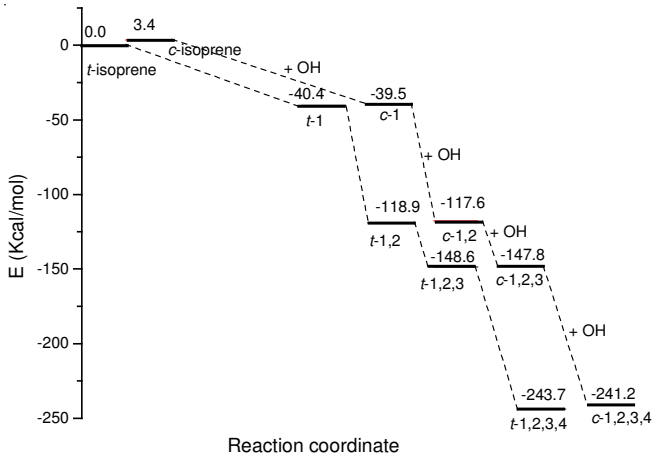

Fig. 7. Schematic potential energy surfaces of multi-step addition reaction at the B3LYP/6-311++G(3df,2pd)||6-31+G** level (a) The system of *trans*-isoprene with OH, (b) The system of *cis*-isoprene with OH

Methylbutenediol: When OH radical continues to react with those adducts of isoprene-OH, the adding position of the second OH group is affected by the first OH group. Concretely speaking, since a p-π conjugate system is formed between the free electron and the C=C double bond in the adduct *t*/*c*-1, the second OH group can be added to C2 position or C4 position which induces to two products, *t*/*c*-1,2 and *t*/*c*-1,4. Similarly, *t*/*c*-1,4 and *t*/*c*-3,4 can be obtained from the addition of *t*/*c*-4 with OH group. As for *t*/*c*-2 and *t*/*c*-3, OH group can only be added to C1 and C4 position and *t*/*c*-1,2 and *t*/*c*-3,4 is formed, respectively. The *t*/*c*-1,2 are more stable than *t*/*c*-1,4 and *t*/*c*-3,4 and the geometry parameters of those methylbutenediols are listed in Fig. 6.

Methylbutanetriol radicals: The subsequent additions of OH group to these methylbutenediol lead to the formation of eight methylbutanetriol radicals, *t*/*c*-1,2,3 and *t*/*c*-1,2,4 originating from the addition of OH to *t*/*c*-1,2 and *t*/*c*-1,3,4 and *t*/*c*-2,3,4 that are obtained after addition of OH to *t*/*c*-3,4. And that *t*/*c*-1,2,4 and *t*/*c*-1,3,4 can also be obtained from the addition of OH to *t*/*c*-1,4. Among the polyols obtained from the addition of *t*-isomers with OH, *t*-1,2,3 is more stable than the others. While *c*-1,2,3 is more stable than other polyols obtained from the addition of *c*-isomers with OH. What's more, *t*-1,2,3 is the most stable isomer among the eight butanetriol radicals. The geometry parameters of those methylbutanetriol radicals, *t*/*c*-1,2,3, are listed in Fig. 6.

Methylbutanetetraols: In the last step, the additions of OH group to these methylbutanetriol radicals lead to the formation of methylbutanetetraols, which are labeled as *t*/*c*-1,2,3,4 (Fig. 2). The *t*-1,2,3,4 has the lowest energy among all the isomers. Those polyols have low vapour pressure and strong polarity allowing them to condense onto preexisting particles and hydrate in aqueous phase. The geometry parameters of t *t*/*c*-1,2,3,4 are listed in Fig. 6.

Equilibrium distributions: The equilibrium distributions of all the available minima are calculated according to eqn. 1. For those *t*-methylbuteneol radicals, the equilibrium distributions of the available minima obtained from the same adding position from C1 to C4 is 0.62:0.28:0.10, 0.20:0.41:0.39, 0.58:0.22:0.20 and 0.52:0.23:0.25. As for *c*-methylbuteneol radicals, the ratios are 0.19:0.65:0.16, 0.36:0.56:0.08, 0.09:0.57:0.34 and 0.62:0.28:0.10. The isomers with the lowest energy at the same adding position almost take the most proportion, so the isomers with the lowest energy at the same adding position are reported only in the subsequent reaction. The ratios of methylbuteneol radicals *t*-1:*t*-2:*t*-3:*t*-4 and *c*-1:*c*-2:*c*-3:*c*-4 are 0.99:0.0: 0.0:0.01 and 0.81:0.0:0.0:0.19, respectively. As for methylbutenediol, the equilibrium distributions of *t*-1,2:*t*-1,4:*t*-3,4 and *c*-1,2:*c*-1,4:*c*-3,4 are 0.31:0.01: 0.68 and 0.88:0.02:0.10. In the subsequent reaction, the ratios of methylbutanetriol radicals *t*-1,2,3:*t*-1,2,4:*t*-1,3,4:*t*-2,3,4 and *c*-1,2,3:*c*-1,2,4:*c*-1,3,4: *c*-2,3,4 are 0.61:0.04:0.27:0.08 and 0.06:0.04:0.82:0.08.

Equilibrium constants: Tang *et al.*[37] in their report about SOA using quantum mechanics method, it has been pointed that the predictive power of quantum mechanics methods can be of great use for species that not been studied experimentally which can make up the scarcity of the experimental data and the estimated methods.

A summary of the reaction pathway for the polyol heterogeneous reactions is given in Fig. 8. The whole process suggested that path *t*-1, *t*-1,2, *t*-1,2,3, to *t*-1,2,3,4 is more favourable than other paths. Zero point energy (E_{zpe}), total energies (E_{total}), enthalpies (H), Gibbs free energies of formation (G), entropy (S) of stationary points are calculated using quantum mechanics method (Table-3). Enthalpies of reaction (ΔH_r^0 (gas)), Gibbs free energies of reaction in gas and hydration reaction in aqueous phases (ΔG_r^0 (gas) and ΔG_r^0 (aq)) are calculated and shown in Table-4. Hydration are more favourable for methylbuteneol radicals, methylbutenediol, methylbutane-tetraol than for methylbutanetriols radicals, shown by the calculated ΔH_r^0 and ΔG_r^0. Equilibrium constants in the gas-phase [reported as

TABLE-3
TOTAL ENERGIES (a.u.), ZPVE (a.u.), ENTHALPIES (a.u.), GIBBS FREE ENERGIES (a.u.), ENTROPY (cal/(mol .k)) OF STATIONARY POINTS ON THE REACTIONS OF OH ADDING TO ISOPRENE

	E_{zpe}	E_{total}	H	G	S
OH	0.00844	-75.73058	-75.72727	-75.74751	42.60
trans-Isoprene	0.11342	-195.21839	-195.21159	-195.24687	74.26
trans-1	0.12794	-271.00830	-270.99968	-271.04063	86.19
trans-1,2	0.14623	-346.85431	-346.84508	-346.88625	86.64
trans-1,2,3	0.16020	-422.62925	-422.61844	-422.66350	94.82
trans-1,2,3,4	0.18027	-498.49971	-498.48818	-498.53485	98.21
cis-Isoprene	0.11293	-195.21936	-195.20697	-195.24404	-75.482
cis-1	0.12795	-271.00689	-270.99828	-271.03920	86.11
cis-1,2	0.14604	-346.85283	-346.84342	-346.88506	87.62
cis-1,2,3	0.15944	-422.62760	-422.61647	-422.66222	96.30
cis-1,2,3,4	0.17960	-498.49598	-498.48411	-498.53143	99.60

TABLE-4
ENTHALPIES, FREE ENERGIES AND EQUILIBRIUM CONSTANTS (REPORTED AS log K) OF REACTIONS IN THE GAS-HASE AND AQUEOUS-PHASE AT THE STANDARD STATE

	Gas-phase			Aqueous-phase	
	ΔH_r	ΔG_r	log K	ΔG_r	log K
(1)	-38.23	-29.02	1.69	-29.71	1.70
(2)	-74.13	-61.56	2.02	-58.44	1.99
(3)	-28.92	-18.66	1.50	-17.08	1.46
(4)	-89.40	-77.71	2.11	-75.63	2.11
(5)	-40.19	-30.65	1.71	-30.95	1.72
(6)	-73.96	-61.71	2.01	-60.13	2.00
(7)	-28.73	-18.61	1.49	-17.05	1.46
(8)	-88.08	-76.37	2.11	-75.21	2.11

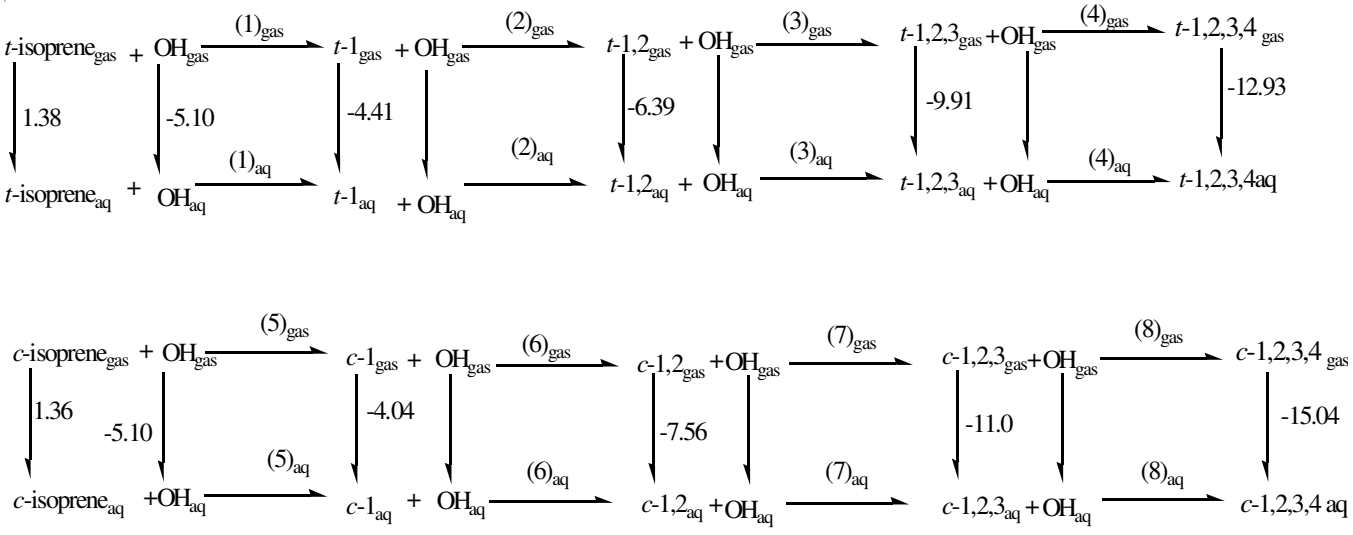

Fig. 8. Pathways for multi-step adding reaction and solvation energies of stationary points were shown. All values are in Kcal/mol (a) The system of *trans*-isoprene with OH, (b) The system of *cis*-isoprene with OH

log K (gas)] and in aqueous solution [log K (aq)] are calculated and shown in Table-4. The quantum calculated log K (gas) values follow the same trend as the estimated log K (aq) for hydration reaction. Results show that the hydration reactions for methylbuteneol radicals, methyl-butenediols, methylbutanetriol radicals and methylbutanetetraols are all thermodynamic favourable.

Conclusion

In this paper, a theoretical study on the important atmospheric reaction of isoprene with OH radical is presented. The comprehensive mechanism study is performed at the QCISD(T)||B3LYP/6-31+G** and B3lYP/6-311++G (3df,2pd)||6-31+G** level including the isomerization of *t/c*-isoprene, the OH-initiated oxidation reactions of isoprene, OH migration reactions of the isomers of the isoprene-OH adducts and the main adducts in the subsequent reaction, such as, methylbuteneol radicals, methylbutenediols, methylbutanetriol radicals and methylbutanetetraols.

Since the potential barrier of the isomerization of *t/c*-isoprene is not high and *c*-isoprene is stable, the isomer of *c*-isoprene should be taken into account when OH-initiated oxidation reactions of isoprene are researched. It is helpful to interpret the formation of 3-methylfuran in the subsequent reactions.

The OH-initiated adducts at the terminal carbons of *t/c*-isoprene allows the radical center to be delocalized, which interpret the stability of the corresponding isomers. The stable sequence should be *t*-1, *c*-1, *t*-4, *c*-4 according to the thermochemistry stability. Compared to energy of OH-*c*-isoprene, the energies of add adducts, even the migration transition states TS12 and TS12a are lower and other migration transition states have a low potential barrier. Then the addition reaction and OH migration reaction occur easily, *i.e.*, all adducts should be obtained in the first step. As for the subsequent addition reaction, a number of isomers exit for the stereochemistry of OH group. And each step is thermodynamic favourable till the formation of methylbutanetetraols. Other mechanisms and kinetic study will be performed later.

ACKNOWLEDGEMENTS

This work is supported by National Natural Science Foundation of China (No. 20903062, No. 20873074 and No. 20737001), Natural Science Foundation of Shandong Province (No. Q2008B07), Independent Innovation Foundation of Shandong University (No. 2010TS064) and Open Project from State Key Laboratory of Environmental Chemistry and Ecotoxicology, Research Center for Eco-Environmental Sciences, Chinese Academy of Sciences (No. KF2009-10).

REFERENCES

1. R. Atkinson, *J. Phys. Chem. Ref. Data*, **2**, 1 (1994).
2. J.H. Seinfeld and S.N. Pandis, Atmospheric Chemistry and Physics: From Air Pollution to Climate Change, John Wiley & Sons: New York (1997).
3. F. Arnold, G. Knop and H. Zeiereis, *Nature*, **321**, 505 (1986).
4. R.A. Cox, R.G. Derwent and M.R. Williams, *Environ. Sci. Technol.*, **14**, 57.
5. T.E. Kleindlenst, G.W. Harris and J.N. Pitts Jr., *Environ. Sci. Technol.*, **16**, 844 (1982).
6. R. Atkinson, S.M. Aschmann, A.M. Winer and J.N. Pitts Jr., *Int. J. Chem. Kinet.*, **14**, 507 (1982).
7. T. Ohta, *J. Phys. Chem.*, **87**, 1209 (1983).
8. P. Campuzano-Just, M.B. Williams and L. D'Ottone, *J. Hynes, Geophys. Res. Lett.*, **27**, 693 (2000).
9. P. Stevens, D. L'Esperance, B. Chuong and G. Martin, *Int. J. Chem. Kinet.*, **31**, 637 (1999).
10. B. Chuong and P. Stevens, *J. Phys. Chem.*, **104**, 5230 (2000).
11. W.S. McGivern, I. Suh, A.D. Clinkenbeard, R. Zhang and S.W. North, *J. Phys. Chem.*, **104**, 6609 (2000).
12. A.C. Lloyd, R. Atkinson, F.W. Lurmann and B. Nitta, *Atmos. Environ.*, **17**, 1931 (1983).
13. J.P. Killus and G.Z. Whitten, *Environ. Sci. Technol.*, **18**, 142 (1984).
14. R. Atkinson, S.M. Aschmann, E.C. Touazon, J. Arey and B. Zielinska, *Int. J. Chem. Kinet.*, **21**, 593 (1989).
15. C.I. Gu, C.M. Rynard, D.G. Hendry and T. Mill, *Environ. Sci. Technol.*, **19**, 151 (1985).
16. E.C. Tuazon and R. Atkinson, *Int. J. Chem. Kinet.*, **22**, 1221(1990).
17. S.E. Paulson and J.H. Seinfeld, *Int. J. Chem. Kinet.*, **24**, 79 (1992).
18. D. Grosjean, *Environ. Sci. Technol.*, **27**, 830 (1993).
19. E.S. Kwok, R. Atkinson and J. Arey, *Environ. Sci. Technol.*, **29**, 2467 (1995).
20. W.F. Lei, R.Y. Zhang, W.S. McGivern, A.D. Kovacs and S.W. North, *Chem. Phys. Lett.*, **326**, 109 (2000).

21. W.F. Lei, A.D. Kovacs and R.Y. Zhang, *J. Chem. Phys.*, **113**, 5354 (2000).
22. W.S. McGivern, I. Suh, A.D. Kovacs, R.Y. Zhang and S.W. North, *J. Phys. Chem. A*, **104**, 6609 (2000).
23. W.F. Lei, R.Y. Zhang, W.S. McGivern, A.D. Kovacs and S.W. North, *J. Phys. Chem. A*, **105**, 471 (2001).
24. D. Zhang and R.Y. Zhang, *J. Am. Chem. Soc.*, **124**, 2692 (2002).
25. D. Zhang, R.Y. Zhang, J. Park and S.W. North, *J. Am. Chem. Soc.*, **124**, 9600 (2002).
26. J. Zhao, R.Y. Zhang, E.C. Fortner and S.W. North, *J. Am. Chem. Soc.*, **126**, 2686 (2004).
27. D. Zhang, R.Y. Zhang and S.W. North, *J. Phys. Chem. A*, **107**, 11013 (2003).
28. J. Park, C.G. Jongsma, R.Y. Zhang and S.W. North, *J. Phys. Chem. A*, **108**, 10688 (2004).
29. M.F. Marquez, I.R. Idaboy, A. Galano and A.V. Bunge, *Environ. Sci. Technol.*, **39**, 8797 (2005).
30. M. Claeys, B. Graham, G. Vas, W. Wang, R. Vermeylen, V. Pashynska, J. Cafmeyer, P. Guyon, M.O. Andreae, P. Artaxo and W. Maenhaut, *Science*, **303**, 1173 (2004).
31. N.S. Handy, J.T. Hynes, L. Bogdan, in eds.: D.J. Bicout and M.J. Field, Quantum Mechanical Simulation Methods for Studying Biological Systems, Les Houches Workshop, pp. 1-27 (1995).
32. W.L. Zhu, H.L. Jiang, K.X. Chen, R.Y. Ji and Y. Cang, *Prog. Chem.*, **11**, 247 (1999).
33. W.L. Zhu, H.L. Jiang, J.Z. Chen, J.D. Gu, K.X. Chen, Y. Cang and R.Y. Ji, *Sci. Chin. (Ser. B)*, **41**, 616 (1998).
34. J.D. Gu, H.L. Jiang, W.L. Zhu, J.Z. Chen, K.X. Chen and R.Y. Ji, *J. Mol. Struct. (Theochem.)*, **459**, 103 (1999).
35. R.Q. Zhang, Y.X. Bu, S.T. Li, J.H. Huang, K.L. Han and G.Z. He, *Sci. Chin. (Ser. B-Chem.)*, **30**, 419 (2000).
36. M.J. Frisch, G.W. Trucks, C. Gonzalez and J.A. Pople, Gaussian, Revision B.03; Pittsburgh PA (2003).
37. C.H. Tong, M. Blanco, W.A. Goddard III and J.H. Seinfeld, *Environ. Sci. Technol.*, **40**, 2333 (2006).
38. V. Barone, M. Cossi and J. Tomasi, *J. Comp. Chem.*, **19**, 404 (1998).
39. V. Barone and M. Cossi, *J. Phys. Chem. A*, **102**, 1995 (1998).